

# 1 **A DNA aptamer that inhibits the formation of unliganded receptor dimer and** 2 **ligand-independent signaling in cancer cells**

3 Akihiro Eguchi,<sup>[a]</sup> Ayaka Ueki,<sup>[a]</sup> Junya Hoshiyama,<sup>[a]</sup> Keiko Kuwata,<sup>[b]</sup> Satoru Nagatoishi,<sup>[c]</sup> Kouhei  
4 Tsumoto,<sup>[a,c,d]</sup> Ryosuke Ueki,<sup>\*[a]</sup> and Shinsuke Sando<sup>\*[a,d]</sup>

5 *[a]Department of Chemistry and Biotechnology, Graduate School of Engineering, The University of*  
6 *Tokyo, 7-3-1, Hongo, Bunkyo-ku, Tokyo 113-8656, Japan. [b]Institute of Transformative Bio-Molecules*  
7 *(WPI-ITbM), Nagoya University, Furo-cho, Chikusa-ku, Nagoya, Aichi 464-8601, Japan. [c]The Insti-*  
8 *tute of Medical Science, The University of Tokyo, 4-6-1 Shirokanedai, Minato-ku, Tokyo 108-8639, Ja-*  
9 *pan. [d]Department of Bioengineering, Graduate School of Engineering, The University of Tokyo, 7-3-1*  
10 *Hongo, Bunkyo-ku, Tokyo 113-8656, Japan.*

11

## 12 **ABSTRACT**

13 Growth factor receptors are activated through dimerization by the binding of their ligands and play  
14 pivotal roles in normal cell function. However, in cancer cells, the overexpression of receptors often  
15 causes the formation of unliganded receptor dimers, which can be activated in a ligand-independent  
16 manner. Thus, the unliganded receptor dimer is a promising target to inhibit aberrant signaling in cancer.  
17 Here, we report an aptamer that inhibits ligand-independent receptor activation via preventing the  
18 formation of unliganded receptor dimer. By biasing the receptor monomer–dimer equilibrium to the  
19 monomer, this aptamer inhibited aberrant cell signaling caused by the unliganded receptor dimer. This  
20 work presents a new possibility of oligonucleotide-based therapeutics for cancer.

21

## 22 **MAIN TEXT**

23 Growth factor receptors (GFRs) transduce cell signaling through activation and dimerization by the  
24 binding of their ligands. Receptor dimerization, a pivotal trigger in signal transduction, brings intracellu-  
25 lar tyrosine kinase domains closer to induce their autophosphorylation. Signaling proteins are recruited  
26 to the phosphorylated sites and transduce cell signaling to the nucleus. Finally, cellular responses, such  
27 as growth and migration, are induced.<sup>1-3</sup> Although the dimerization and activation of the GFRs are  
28 strictly regulated by the binding of their ligands, GFRs can form ligand-independent receptor dimers  
29 and be activated in a ligand-independent manner (Figure 1a).<sup>4-6</sup> In particular, the formation of un-  
30 liganded dimers occurs frequently in GFR-overexpressing cancer cells because the overexpression of  
31 GFR increases the density of receptors on the cell membrane. Importantly, their ligand-independent

1 aberrant activity promotes cancer malignancy. The  
2 formation of unliganded receptor dimers plays a  
3 key role in cancer development; thus, this could be  
4 a promising target for cancer therapy.<sup>4-6</sup>

5 The inhibition of receptor dimerization is a  
6 major strategy for the treatment of the aberrant  
7 activity of GFRs. Antagonists that block the lig-  
8 and-receptor interactions are good examples of  
9 dimerization inhibitors (DIs) that inhibit ligand-  
10 dependent receptor activation. However, DIs gen-  
11 erally do not function as inhibitors of ligand-  
12 independent receptor activation. To inhibit ligand-  
13 independent receptor activation, unliganded di-  
14 merization inhibitors (UDIs) that can block the  
15 receptor-receptor interactions are necessary. For

16 example, trastuzumab, an anti-human epidermal growth factor receptor 2 (HER2) antibody, is known as  
17 one of the representative UDIs.<sup>7,8</sup> It has been proposed that trastuzumab inhibits the formation of un-  
18 liganded receptor dimers by binding to the dimer interface between HER2 and other epidermal growth  
19 factor receptor family members and prevents the ligand-independent activation of the receptors in can-  
20 cer cells.<sup>7,8</sup> This antibody has demonstrated the therapeutic potential of UDIs, and thus, the development  
21 of novel UDIs based on other chemical entities would be of great interest in anti-cancer therapy.

22 We have accepted the challenge to design a nucleic acid aptamer that can prevent the formation of  
23 unliganded dimers and inhibit the ligand-independent aberrant activation of a GFR (Figure 1b). Ap-  
24 tamers have attracted attention as a chemical alternative to antibodies. In addition to their affinity and  
25 specificity, comparable to those of antibodies, aptamers have advantages in thermal stability, quality  
26 uniformity, and ease of preparation.<sup>9</sup> Various aptamers have been reported as receptor binders, including  
27 as antagonists<sup>10-15</sup> and agonists<sup>15-20</sup> for GFRs. Although several reports have demonstrated that aptamers  
28 are useful for the inhibition of the ligand-dependent receptor activation, there are still significant barriers  
29 to the inhibition of the ligand-independent activation. An aptamer for the AXL receptor, a type of  
30 GFRs, inhibited the activation of the AXL receptor overexpressed in a cancer cell.<sup>13</sup> This aptamer may  
31 inhibit the ligand-independent receptor activation, but the mechanism of action remains unclear.

32 In this study, we report the demonstration of the aptamer that functions as a UDI, exerting the inhibi-  
33 tion of the ligand-independent GFR activation. Our DNA aptamer, named Apt\_46, inhibits the un-

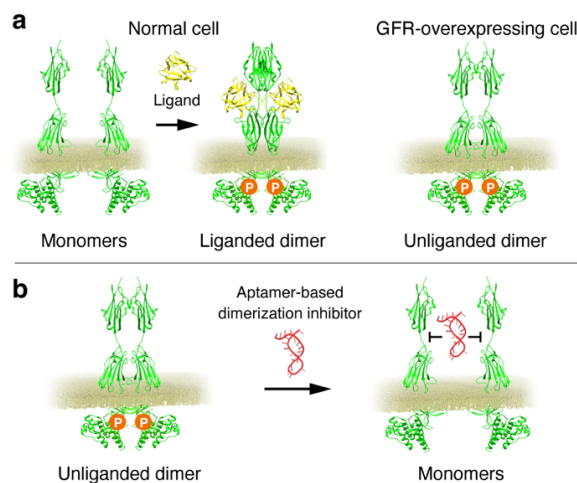


**Figure 1.** Schematic representation of the activation of growth factor receptor (GFR) and its inhibition. (a) GFRs are dimerized and phosphorylated by the binding of their cognate ligands. GFR-overexpression causes unliganded dimer formation and aberrant activation in cancer cells. (b) DNA aptamer that works as an inhibitor of the unliganded dimerization of GFRs. The schematic images of the receptor and ligand are depicted using data from the Protein Data Bank (PDB IDs: 3OJM and 5UR1).

1 liganded dimer formation of fibroblast growth factor receptor (FGFR) 2b, overexpressed in a cancer cell.  
2 The inhibition of the formation of unliganded receptor dimers by Apt\_46 prevents the aberrant activity  
3 of FGFR2b and downstream signaling proteins with high specificity. This study shows that DNA ap-  
4 tamers can indeed function as UDIs and a DNA aptamer-based UDI could be a novel class of oligonu-  
5 cleotide therapeutics.

6 The FGFR family is composed of four members (FGFR1–4) and their cognate ligands, fibroblast  
7 growth factors (FGFs), comprise a 22-member family (FGF1–14 and FGF16–23).<sup>21</sup> Except FGFR4,  
8 FGFRs produce two splicing variants, called IIIb and IIIc form, in which a loop in Ig-like domain 3 is  
9 encoded by different exons.<sup>21</sup> Each FGFR member is specifically expressed in various tissues and plays  
10 an important role in the regulation of tissue- and cell-specific proliferation and development through its  
11 characteristic interaction with FGFs.<sup>21</sup>

12 FGFRs are also prominent oncogenes that are frequently overexpressed and ligand-independently ac-  
13 tivated in various cancers. As the expression profile of each FGFR type shows a distinct pattern in tis-  
14 sues and cell types, it is necessary to specifically inhibit only the target member of the FGFR family  
15 without affecting the activities of other FGFRs (Figure 2a). In the case of FGFR2b, gene amplification,  
16 receptor overexpression, and ligand-independent activation of FGFR2b are observed in a variety of can-  
17 cer cells, such as liver, colorectal, and gastric cancers.<sup>6,22–25</sup> Although some tyrosine kinase inhibitor  
18 drugs against FGFRs, such as AZD4547 and BGJ398,<sup>26–29</sup> have been developed and are under clinical  
19 trials, these also inhibit other FGFR family members owing to the reduced specificity caused by the  
20 structural similarity of the kinase domain of FGFRs. Therefore, the development of UDIs specific for  
21 FGFR2b is of great significance.

22 We first selected an FGFR2b-binding DNA aptamer *in vitro* based on the systematic evolution of  
23 ligands by exponential enrichment (SELEX) as previously reported.<sup>18</sup> The selection was conducted us-  
24 ing an N<sub>40</sub> random DNA pool. After six rounds of selection, a 76-mer sequence was identified as a po-  
25 tential FGFR2b binder and named Apt\_76 (Figure 2b). We next truncated Apt\_76 into a minimal bind-  
26 ing motif. As various DNA aptamers have been reported to adopt G-quadruplex (G4) structures,<sup>12,30–32</sup>  
27 we hypothesized that some guanine-tracts in the sequence would form a G4 structure and contribute to  
28 receptor binding. The analysis using QGRS Mapper<sup>33</sup> predicted the presence of a G4 structure within  
29 the sequence of Apt\_76 (Figure 2b). The formation of the G4 structure was assessed using circular di-  
30 chroism (CD) measurements in the presence or absence of potassium ions. The CD spectra of Apt\_76  
31 showed a positive peak at 265 nm and negative peak at 240 nm (left in Figure 2c) that were enhanced in  
32 the presence of potassium ions, which suggests the formation of a parallel G4 structure.<sup>34</sup> We then syn-  
33 thesized several truncates of Apt\_76 containing or not containing the predicted G4-forming sequence

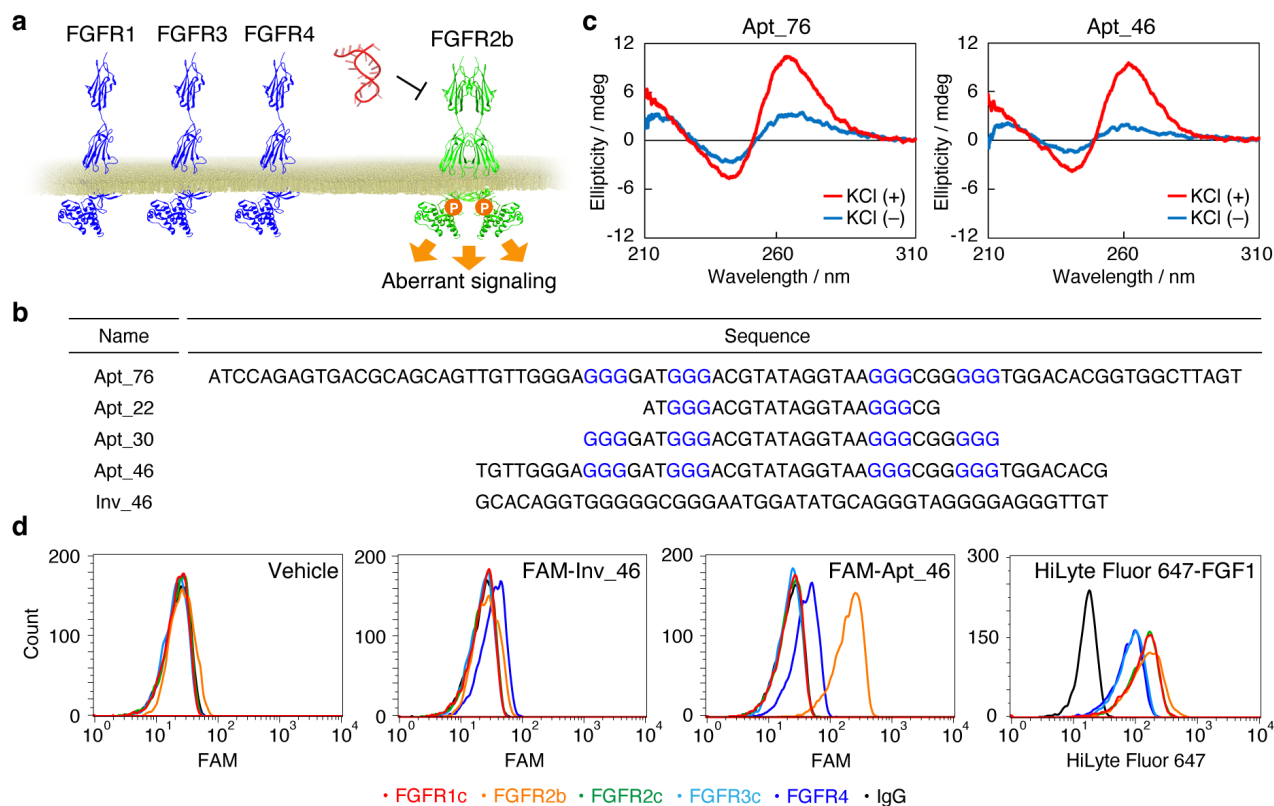


**Figure 2.** Selection and evaluation of an FGFR2b-binding DNA aptamer. (a) Schematic representation of aberrant signaling of overexpressed FGFR2b and its inhibition with an FGFR2b-selective DNA aptamer. (b) Full-length and truncated sequences of the FGFR2b-binding DNA aptamer candidates. G-tracts that are predicted to form a G4 structure by QGRS mapper are depicted in blue. (c) CD spectra of Apt\_76 (left) and Apt\_46 (right). Oligonucleotide samples (5  $\mu$ M) were refolded in 20 mM Tris-HCl (pH 7.6) with (red) or without (blue) KCl (100 mM) and subjected to CD measurement at 37  $^{\circ}$ C. (d) FAM-labeled oligonucleotide samples (100 nM) or HiLyte Fluor 647-labeled FGF1 (100 nM) was incubated with FGFRs-Fc- or IgG-immobilized magnet beads for 15 min at ambient temperature. The fluorescent signal from FGFR-bound ligands was measured using flow cytometry.

1 (Apt\_22, Apt\_30, and Apt\_46 in Figure 2b). Among them, only Apt\_46 showed binding to FGFR2b  
 2 (Figure S1) and CD spectra similar to those of Apt\_76 (right in Figure 2c), whereas the ellipticity of  
 3 Apt\_30 and Apt\_22 decreased in accordance with truncation (Figure S2). From these results, we used  
 4 Apt\_46 as a minimal FGFR2b-binding motif for further experiments.

5 Next, the binding specificity of Apt\_46 to FGFR2b was assessed. Protein G-conjugated magnetic  
 6 beads were incubated with an Fc-chimera of FGFR1c, 2b, 2c, 3c, and 4. Human IgG was used as a nega-  
 7 tive control bead. These beads were subsequently incubated with FAM-labeled Apt\_46, its inversed  
 8 sequence (Inv\_46 in Figure 2b), or HiLyte Fluor 647-labeled FGF1. FGF1 is a universal ligand against  
 9 all FGFRs;<sup>21</sup> therefore, it was used as a positive control ligand for all FGFRs. Apt\_46 showed specific  
 10 binding to FGFR2b, whereas FGF1 bound to all FGFR family members (Figure 2d). Although a small  
 11 amount of FGFR4 binding was observed, a similar trend was observed in Inv\_46, which suggests that  
 12 FGFR4 interacts with these oligonucleotides in a nonspecific manner.

1 We then explored the binding epitope of  
 2 Apt\_46 on FGFR2b. A competitive binding assay  
 3 was performed using FGF10, a specific ligand for  
 4 FGFR2b, the binding site for which on FGFR2b  
 5 was revealed by X-ray crystallography (Figure  
 6 S3).<sup>35</sup> The binding of FGF10 to FGFR2b de-  
 7 creased as the concentration of Apt\_46 increased  
 8 (Figure 3a), which suggests that the epitope of  
 9 Apt\_46 overlaps with that of FGF10. We con-  
 10 structed a putative dimer model of FGF10-bound  
 11 FGFR2b, in which two FGF10–FGFR2b com-  
 12 plexes (PDB ID: 1NUN) were superimposed on a  
 13 known dimer structure of FGF2-bound FGFR1c  
 14 (PDB ID: 1FQ9) (Figure 3b and S3). According  
 15 to this structural model, FGF10 should be bound  
 16 on the opposite side of the dimer interface located  
 17 in Ig-like domains 2 and 3.<sup>36</sup> As Apt\_46 did not  
 18 bind to FGFR2c (Figure 2d), which is a splicing  
 19 variant of FGFR2b at Ig-like domain 3 (orange-  
 20 colored region in Figure 3b and sequence in Fig-  
 21 ure S4), Ig-like domain 3 is the most likely region  
 22 where Apt\_46 binds.

23 The thermodynamic parameters of Apt\_46  
 24 binding to FGFR2b were measured using iso-  
 25 thermal titration calorimetry (Figure 3c). The dis-  
 26 sociation constant ( $K_D$ ) was  $79.7 \pm 16.7$  nM and  
 27 the titration curve showed a large enthalpy gain

28 ( $\Delta H = -20.2 \pm 0.5$  kcal/mol) and entropy loss ( $-T\Delta S = 10.5 \pm 0.6$  kcal/mol). This result suggests that  
 29 hydrogen bonds and electrostatic interactions are formed in the FGFR2b–Apt\_46 interaction, which  
 30 may contribute to the specific binding of the aptamer.

31 During the characterization of Apt\_46, we unexpectedly observed that Apt\_46 dissociated the un-  
 32 liganded FGFR2b dimers on the cell surface. FGFR2b-overexpressing gastric cancer SNU16 cells<sup>37</sup>  
 33 were incubated with Apt\_46 followed by incubation with the crosslinking agent

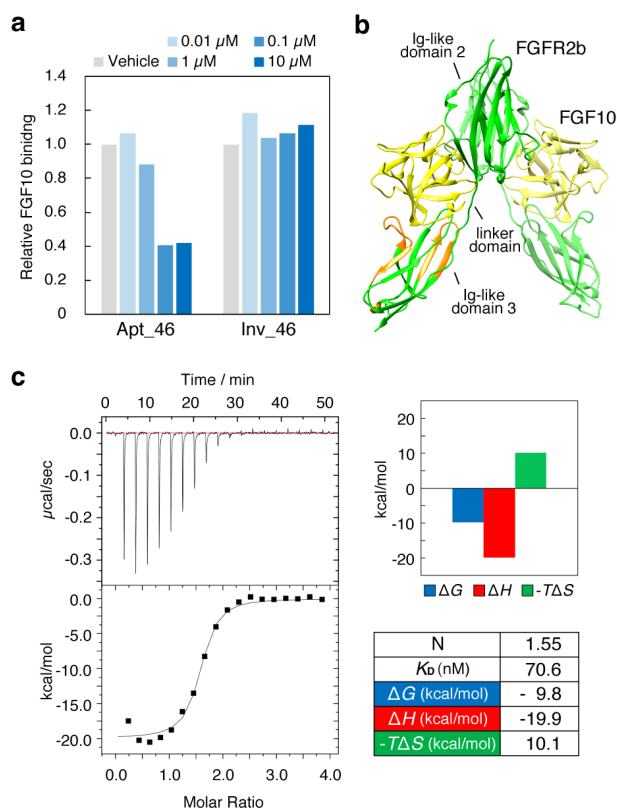


**Figure 3.** Characterizations of binding fashion of Apt\_46 to FGFR2b. (a) Competition assay of FGF10 and Apt\_46. HiLyte Fluor 647-labeled FGF10 (0.1  $\mu\text{M}$ ) and FAM-labeled oligonucleotide samples (0.01–10  $\mu\text{M}$ ) were co-incubated with FGFR2b-Fc-immobilized magnet beads for 15 min at ambient temperature. The fluorescent signal of HiLyte Fluor 647-labeled FGF10 bound to the beads was measured using flow cytometry. (b) Putative model of FGFR2b dimer (green) induced by FGF10 (yellow) binding. A part of Ig-like domain 3 (orange) is encoded by different exons in FGFR2b and FGFR2c. The FGFR2b dimer complex model is built by superimposing FGFR2b–FGF10 complex structure (PDB ID: 1NUN) on a known FGFR1c–FGF2 dimer structure (PDB ID: 1FQ9). (c) Isothermal titration calorimetry measurements were conducted in Dulbecco’s phosphate-buffered saline at 25 °C. The profile was obtained by the sequential titration of Apt\_46 (80–100  $\mu\text{M}$ ) to a solution of recombinant FGFR2b extracellular domain (4  $\mu\text{M}$ ). The parameters are shown as the mean of three measurements  $\pm$  SD. The representative titration curve is shown.

1 bis(sulfosuccinimidyl)suberate (BS3). FGFR2b was crosslinked in the absence of the FGF ligand, which  
 2 suggests the formation of an unliganded FGFR2b dimer (Figure 4a). However, when the crosslink was  
 3 performed in the presence of Apt\_46, the dimer fraction was almost completely reduced, whereas incu-  
 4 bation with Inv\_46 did not affect the crosslinking pattern. The result indicates that the equilibrium of the  
 5 monomeric–dimeric receptor was biased to the monomeric one. Thus, we concluded that Apt\_46 inhib-  
 6 its the unliganded dimer formation of FGFR2b.

7 As the formation of unliganded dimers is associated with the aberrant activation of receptors, we  
 8 analyzed whether Apt\_46 also inhibited the autophosphorylation of FGFR2b in SNU16 cells. The phos-  
 9 phorylation of the intracellular domain of FGFR2b was analyzed by label-free quantitative liquid chro-  
 10 matography-tandem mass spectrometry (LC-MS/MS) measurements. Among the phosphorylation sites  
 11 of FGFR2b detected in both Apt\_46-treated and vehicle-treated samples (Figure 4b), we focused on the  
 12 phosphorylated Y586/588, Y656/657, and S780.<sup>38,39</sup> Y656/657 is located in the activation loop of the

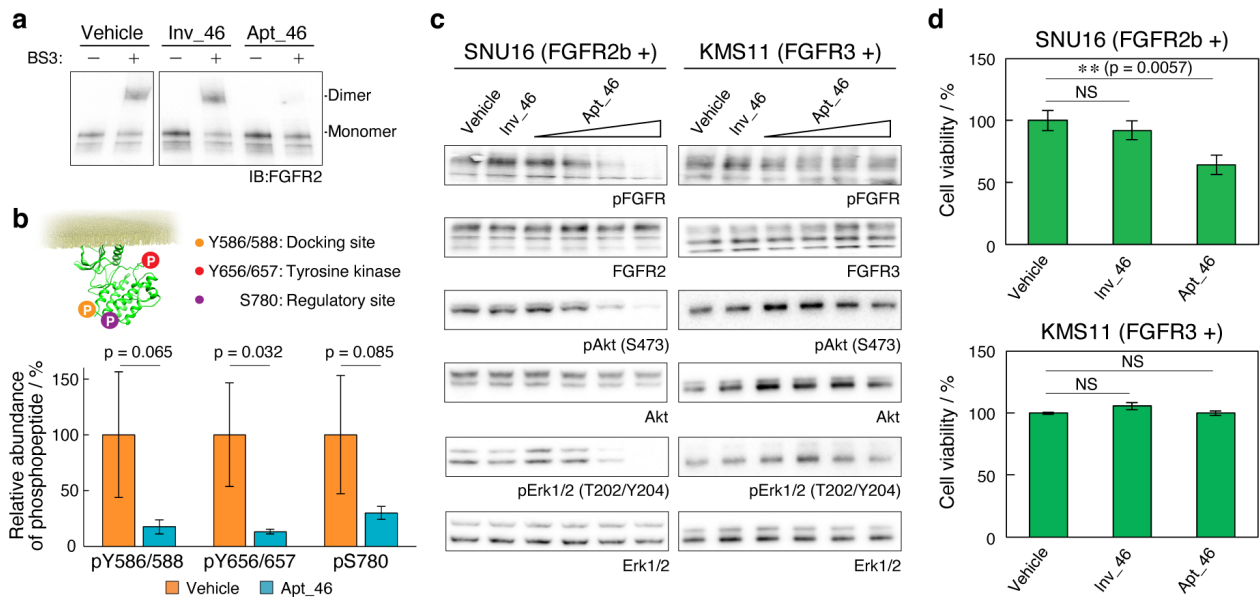


**Figure 4.** Inhibitory effect of Apt\_46 on the formation of unliganded dimer and aberrant cell signaling. (a) Western blotting analysis of crosslinked FGFR2b dimer. SNU16 was incubated with Apt\_46 (1  $\mu$ M) or Inv\_46 (1  $\mu$ M) for 1 h on ice, followed by crosslinking with BS3 (500  $\mu$ M) for 1 h on ice. The cell lysates were used for Western blotting and FGFR2b was detected. The uncropped image is shown in Figure S5. (b) Phosphorylation level of FGFR2b intracellular domain measured by LC-MS/MS analysis. FGFR2b was immunoprecipitated from cell lysates of SNU16 incubated with vehicle or Apt\_46 (1  $\mu$ M). FGFR2b protein was extracted from polyacrylamide gel after SDS-PAGE and digested by Lys-C/Trypsin, followed by LC-MS/MS analysis of phosphopeptides (refer to the supporting information). The bar graph shows mean  $\pm$  SD (N = 3). An unpaired two-tailed t-test was performed between vehicle- and Apt\_46-treated conditions. The schematic illustration of intracellular FGFR2 kinase domain with detected phosphorylation sites is depicted using data from the Protein Data Bank (PDB ID: 2PSQ). (c) Western blotting of cell lysates of SNU16 and KMS11 cells incubated with Apt\_46 (16, 80, 400, and 2000 nM) or Inv\_46 (2000 nM) for 15 min. (d) Growth assay of SNU16 and KMS11 cells. Cells were cultured in the presence of 3'-dT conjugated Inv\_46 or Apt\_46 for 72 h. The initial concentration of the oligonucleotide samples was 1  $\mu$ M and the sample was newly supplemented every 24 h (refer to the supporting information). Cell viability was measured using cell counting kit-8. The bar graph shows mean  $\pm$  SD (N = 3). An unpaired two-tailed t-test was performed between vehicle and Inv\_46- or Apt\_46-treated conditions; \*\*, p < 0.01; NS: p > 0.05.

1 tyrosine kinase domain and its transphosphorylation restores kinase activity. Y586/Y588 and S780 func-  
2 tion as a docking site for signaling proteins and a regulator of FGFR2b activity, respectively. Under the  
3 experimental conditions, the addition of Apt\_46 significantly reduced the phosphorylation levels of  
4 Y656/657 ( $p = 0.032$ ). The dephosphorylation of Y656/657 site is interpreted as the suppression of the  
5 tyrosine kinase activity of FGFR2b by the addition of Apt\_46. This result suggests that the inhibition of  
6 the formation of unliganded receptor dimers by Apt\_46 leads to the inhibition of the tyrosine kinase  
7 activity of FGFR2b.

8 Finally, we investigated the inhibitory effect of Apt\_46 on the aberrant signaling of FGFR2b in can-  
9 cer using the FGFR2b-overexpressing SNU16 cell line. To confirm the selective inhibition of FGFR2b-  
10 dependent signaling, we chose the FGFR3-overexpressing KMS11 cell line<sup>26,40</sup> for comparison (Figure  
11 S6). Because of receptor overexpression, FGFR2 or 3 is autophosphorylated in each cell line.<sup>26,37,40</sup> Spe-  
12 cific binding of Apt\_46 to SNU16 cells was confirmed using flow cytometry (Figure S7). As expected,  
13 the addition of Apt\_46 reduced the ligand-independent phosphorylation of FGFR2b and the downstream  
14 kinases, such as Akt (S473) and Erk1/2 (T202/Y204), in SNU16 cells (Figure 4c), whereas the phos-  
15 phosphorylation of FGFR3 and the downstream kinases in KMS11 cells was almost unaffected. This is in  
16 contrast to the broad inhibitory spectrum of the pan-FGFR kinase inhibitor AZD4547, which inhibited  
17 the phosphorylation of FGFRs in both cell lines (Figure S8). As Apt\_46 inhibited cell growth-related  
18 downstream signaling proteins Akt and Erk, we investigated whether Apt\_46 affects the growth of  
19 SNU16 cells. SNU16 and KMS11 cells were cultured in the presence of Apt\_46 for 72 h and the rela-  
20 tive cell viability was measured (Figure 4d). Under the experimental conditions, the growth of SNU16  
21 cells was significantly inhibited by Apt\_46 ( $p = 0.0057$ ), whereas that of KMS11 cells was not affected  
22 ( $p = 0.50$ ). Consistently, we showed that the inhibitory effect of Apt\_46 on FGFR2b phosphorylation  
23 lasted over several hours under the experimental conditions (Figure S9). Although the effects of oligo-  
24 nucleotides on cell growth need to be analyzed in more detail, this result suggests that Apt\_46 inhibits  
25 cancer cell growth via the inhibition of the dimerization of FGFR2b and the resultant aberrant signaling.

26 In the present study, we report the demonstration of DNA aptamer that functions as a UDI to prevent  
27 the formation of unliganded receptor dimers on cancer cells. This aptamer inhibits the ligand-  
28 independent aberrant activity of GFRs, thereby exerting an inhibitory effect on downstream signaling.

29 The aptamer showed specific binding to FGFR2b (Figure 2d) and successfully inhibited FGFR2b-  
30 dependent intracellular signaling in a specific manner (Figure 4c). Specificity is an important indicator  
31 for the practical application of inhibitors. Tyrosine kinase inhibitors, which are currently major chemo-  
32 therapy medications, often suffer from low specificity owing to the structural similarity of tyrosine ki-  
33 nases. AZD4547, a tyrosine kinase inhibitor of FGFRs, inhibits FGFR1–3 indistinguishably.<sup>28</sup> When we

1 compared the effects of Apt<sub>46</sub> and AZD4547 on  
 2 the intracellular phosphoproteome of SNU16, dif-  
 3 ferent intracellular responses were observed (Fig-  
 4 ure 5 and Table S1). Under the experimental con-  
 5 ditions, we quantified 2,386 phosphopeptides  
 6 (“Quantified” in Figure 5) from 1,140 proteins.  
 7 Among quantified phosphopeptides, there were 89  
 8 phosphopeptides whose SILAC ratio is more than  
 9 2 or less than 0.5 in either or both of Apt<sub>46</sub>-  
 10 treated condition and AZD4547-treated condition  
 11 (“Regulated” in Figure 5). Among the 89 regulat-  
 12 ed phosphopeptides, 31 phosphopeptides showed  
 13 more than two-fold different SILAC ratios be-  
 14 tween the two conditions (“Changed (Apt vs  
 15 AZD)” in Figure 5). Such different effects may be  
 16 explained by the fact that Apt<sub>46</sub>, an oligonucleo-  
 17 tide-based UDI, acts in a receptor-specific manner,  
 18 whereas the tyrosine kinase inhibitor AZD4547  
 19 can cross-react with some intracellular tyrosine

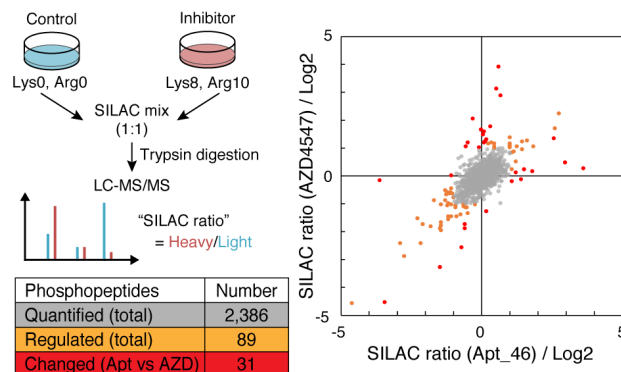


**Figure 5.** Schematic illustration of SILAC (stable isotope labeling by amino acids in cell culture)-based quantitative MS analysis. SNU16 cells grown in heavy SILAC medium were lysed using 8 M guanidium-HCl (pH 8.5) after 15 min incubation with Apt<sub>46</sub> (1 μM) or AZD4547 (1 μM). The cells grown in light SILAC medium were lysed after 15 min incubation with vehicle. The lysates were mixed at a 1:1 mass ratio based on the extracted protein and subjected to quantitative LC-MS/MS measurements. Three independent SILAC samples were prepared. Phosphopeptides that were quantified for a minimum of two of three samples in both conditions are listed. The SILAC ratio of the listed phosphopeptides are plotted in the scatter plot as “Quantified (total)” (gray). The phosphopeptides whose SILAC ratio is more than 2 or less than 0.5 in either or both of Apt<sub>46</sub>-treated condition and AZD4547-treated condition are defined as “Regulated (total)” (orange in the scatter plot). “Regulated” phosphopeptides whose SILAC ratio differs more than twice between Apt<sub>46</sub>-treated and AZD4547-treated conditions are defined as “Changed (Apt vs AZD)” (red in the scatter plot)”.

20 kinases. From these results, UDIs, which are based on specific binders to the extracellular domains of  
 21 their target receptors, are expected to have few side effects and only inhibit their binding targets.

22 Although unliganded receptor dimers are important targets for cancer therapy, the structural basis of  
 23 their formation remains largely unknown. This poses a challenge for the development of UDIs and elu-  
 24 cidation of the mechanism of their action. We revealed that our aptamer binds to the opposite side of the  
 25 ligand-dependent FGFR2b dimer interface (Figure 3a and 3b). However, more information is required  
 26 to elucidate the inhibitory mechanism, although it is beyond the scope of this research. To establish a  
 27 rational design guideline for UDIs, future studies on the structural analysis of unliganded receptor di-  
 28 mers and interaction between aptamers and receptors are expected.

## 30 ACKNOWLEDGMENT

31 The expression vector pEFs<sup>41</sup> was kindly provided by Prof. Yamashita (Yokohama City University).  
 32 The authors thank Dr. Tamura (Kyoto University) for helpful advice about the data analysis of quantita-  
 33 tive proteomics. The authors also thank Dr. Goto and Prof. Suga (The University of Tokyo) for the use

1 of CD spectrometry. This work was supported by grants from the Asahi Glass Foundation for S.S., a  
2 Grant-in-Aid for Young Scientists (#19K15693) from the Japan Society for the Promotion of Science  
3 (JSPS) and a Noguchi-Shitagau Research Grant from The Noguchi Institute for R.U., and partly sup-  
4 ported by AMED under Grant Number JP20ak0101139 for S.S. and JP20am0101094 for K.T. ITbM is  
5 supported by the World Premier International Research Center Initiative, Japan.

6

## 7 AUTHOR INFORMATION

8 Corresponding Authors

9 \*r.ueki@chembio.t.u-tokyo.ac.jp

10 \*ssando@chembio.t.u-tokyo.ac.jp

11

## 12 REFERENCES

- 13 [1] Y. Yarden, A. Ullrich, *Annu. Rev. Biochem.* **1988**, *57*, 443–478.
- 14 [2] L. C. Welsh, *J. Biol. Chem.* **1994**, *269*, 32023–32026.
- 15 [3] S. Bogdan, C. Klämbt, *Curr. Biol.* **2001**, *11*, R292–R295.
- 16 [4] R. Worthylake, L. K. Opresko, H. S. Wiley, *J. Biol. Chem.* **1999**, *274*, 8865–8874.
- 17 [5] N. Shinomiya, C. F. Gao, Q. Xie, M. Gustafson, D. J. Waters, Y. W. Zhang, G. F. V.  
18 Woude, *Cancer Res.* **2004**, *64*, 7962–7970.
- 19 [6] N. Turner, A. Pearson, R. Sharpe, M. Lambros, F. Geyer, M. A. Lopez-Garcia, R. Natrajan, C.  
20 Marchio, E. Iorns, A. Mackay, C. Gillett, A. Grigoriadis, A. Tutt, J. S. Reis-Filho, A. Ash-  
21 worth, *Cancer Res.* **2010**, *70*, 2085–2094.
- 22 [7] M. C. Franklin, K. D. Carey, F. F. Vajdos, D. J. Leahy, A. M. de Vos, M. X. Sliwkowski, *Cancer*  
23 *Cell* **2004**, *5*, 317–328.
- 24 [8] T. T. Junttila, R. W. Akita, K. Parsons, C. Fields, G. D. L. Phillips, L. S. Friedman, D. Sampath, M.  
25 X. Sliwkowski, *Cancer Cell* **2009**, *15*, 429–440.
- 26 [9] J. Zhou, J. Rossi, *Nat. Rev. Drug Discov.* **2017**, *16*, 181–202.
- 27 [10] C. H. B. Chen, G. A. Chernis, V. Q. Hoang, R. Landgraf, *Proc. Natl. Acad. Sci. U. S. A.* **2003**, *100*,  
28 9226–9231.
- 29 [11] N. Li, H. H. Nguyen, M. Byrom, A. D. Ellington, *PLoS One* **2011**, *6*, e20299.
- 30 [12] R. Ueki, S. Sando, *Chem. Commun.* **2014**, *50*, 13131–13134.
- 31 [13] P. Kanlikilicer, B. Ozpolat, B. Aslan, R. Bayraktar, N. Gurbuz, C. Rodriguez-Aguayo, E. Bay-  
32 raktar, M. Denizli, V. Gonzalez-Villasana, C. Ivan, G. L. R. Lokesh, P. Amero, S. Catuogno, M.

- 1 Haemmerle, S. Y. Y. Wu, R. Mitra, D. G. Gorenstein, D. E. Volk, V. de Franciscis, A. K. Sood, G.  
2 Lopez-Berestein, *Mol. Ther. Nucleic Acids* **2017**, *9*, 251–262.
- 3 [14] L. Wang, H. Liang, J. Sun, Y. Liu, J. Li, J. Li, J. Li, H. Yang, *J. Am. Chem. Soc.* **2019**, *141*, 12673–  
4 12681.
- 5 [15] N. Kamatkar, M. Levy, J. M. Hébert, *Mol. Ther. Nucleic Acids* **2019**, *17*, 530–539.
- 6 [16] V. Ramaswamy, A. Monsalve, L. Sautina, M. S. Segal, J. Dobson, J. B. Allen, *Nucleic Acid Ther.*  
7 **2015**, *25*, 227–234.
- 8 [17] R. Ueki, A. Ueki, N. Kanda, S. Sando, *Angew. Chem. Int. Ed.* **2016**, *55*, 579–582.
- 9 [18] R. Ueki, S. Atsuta, A. Ueki, J. Hoshiyama, J. Li, Y. Hayashi, S. Sando, *Chem. Commun.* **2019**, *55*,  
10 2672–2675.
- 11 [19] T. Yoshitomi, M. Hayashi, T. Oguro, K. Kimura, F. Wayama, H. Furusho, K. Yoshimoto, *Mol.*  
12 *Ther. Nucleic Acids* **2020**, *19*, 1145–1152.
- 13 [20] R. Ueki, S. Uchida, N. Kanda, N. Yamada, A. Ueki, M. Akiyama, K. Toh, H. Cabral, S. Sando, *Sci.*  
14 *Adv.* **2020**, *6*, eaay2801.
- 15 [21] D. M. Ornitz, N. Itoh, *WIREs Dev. Biol.* **2015**, *4*, 215–266.
- 16 [22] Y. Katoh, M. Katoh, *Int. J. Mol. Med.* **2009**, *23*, 307–311.
- 17 [23] Y. Matsuda, J. Ueda, T. Ishiwata, *Patholog. Res. Int.* **2012**, *2012*, 574768.
- 18 [24] J. C. Jo, E. K. Choi, J. S. Shin, J. H. Moon, S. W. Hong, H. R. Lee, S. M. Kim, S. A. Jung, D. H.  
19 Lee, S. H. Jung, S. H. Lee, J. E. Kim, K. Kim, Y. S. Hong, Y. A. Suh, S. J. Jang, E. K. Choi, J. S.  
20 Lee, D. H. Jin, T. W. Kim, *Mol. Cancer Ther.* **2015**, *14*, 2613–2622.
- 21 [25] S. Ahn, J. Lee, M. Hong, S. T. Kim, S. H. Park, M. G. Choi, J. H. Lee, T. S. Sohn, J. M. Bae, S.  
22 Kim, S. H. Jung, W. K. Kang, K. M. Kim, *Mod. Pathol.* **2016**, *29*, 1095–1103.
- 23 [26] P. R. Gavine, L. Mooney, E. Kilgour, A. P. Thomas, K. Al-Kadhimi, S. Beck, C. Rooney, T. Cole-  
24 man, D. Baker, M. J. Mellor, A. N. Brooks, T. Klinowska, *Cancer Res.* **2012**, *72*, 2045–2056.
- 25 [27] J. Chang, S. Wang, Z. Zhang, X. Liu, Z. Wu, R. Geng, X. Ge, C. Dai, R. Liu, Q. Zhang, W. Li, J.  
26 Li, *Oncotarget* **2015**, *6*, 2009–2022.
- 27 [28] Y. K. Chae, K. Ranganath, P. S. Hammerman, C. Vaklavas, N. Mohindra, A. Kalyan, M.  
28 Matsangou, R. Costa, B. Carneiro, V. M. Villaflor, M. Cristofanilli, F. J. Giles, *Oncotarget* **2017**, *8*,  
29 16052–16074.
- 30 [29] J. Perez-Garica, E. Muñoz-Couselo, J. Soberino, F. Racca, J. Cortes, *Breast* **2018**, *37*, 126–133.
- 31 [30] R. F. Macaya, P. Schultze, F. W. Smith, J. A. Roe, J. Feigon, *Proc. Natl. Acad. Sci. U. S. A.* **1993**,  
32 *90*, 3745–3749.
- 33 [31] Y. Nonaka, K. Sode, K. Ikebukuro, *Molecules* **2010**, *15*, 215–225.

- 1 [32]H. Fujita, Y. Imaizumi, Y. Kasahara, S. Kitadume, H. Ozaki, M. Kuwahara, N. Sugimoto, *Pharma-*  
2 *ceuticals* **2013**, *6*, 1082–1093.
- 3 [33]O. Kikin, L. D'Antonio, P. S. Bagga, *Nucleic Acids Res.* **2006**, *34*, W676–W682.
- 4 [34]D. M. Gray, J. D. Wen, C. W. Gray, R. Repges, C. Repges, G. Raabe, J. Fleischhau-  
5 *er*, *Chirality* **2008**, *20*, 431–440.
- 6 [35]B. K. Yeh, M. Igarashi, A. V. Eliseenkova, A. N. Plotnikov, I. Sher, D. Ron, S. A. Aaronson, M.  
7 *Mohammadi*, *Proc. Natl. Acad. Sci. U. S. A.* **2003**, *100*, 2266–2271.
- 8 [36]A. Zinkle, M. Mohammadi, *Front. Genet.* **2019**, *10*, 102.
- 9 [37]K. Kunii, L. Davis, J. Gorenstein, H. Hatch, M. Yashiro, A. Di Bacco, C. Elbi, B. Lutter-  
10 *bach*, *Cancer Res.* **2008**, *68*, 2340–2348.
- 11 [38]Y. Luo, C. Yang, C. Jin, R. Xie, F. Wang, W. L. McKeehan, *Cell. Signal.* **2009**, *21*, 1370–1378.
- 12 [39]P. Szybowska, M. Kostas, J. Wesche, A. Wiedlocha, E. M. Haugsten, *Cells* **2019**, *8*, 518.
- 13 [40]V. Chell, K. Balmanno, A. S. Little, M. Wilson, S. Andrews, L. Blockley, M. Hampson, P. R.  
14 *Gavine*, S. J. Cook, *Oncogene* **2013**, *32*, 3059–3070.
- 15 [41]A. López-Perrote, R. Castaño, R. Melero, T. Zamarro, H. Kurosawa, T. Ohnishi, A. Uchiyama, K.  
16 *Aoyagi*, G. Buchwald, N. Kataoka, A. Yamashita, O. Llorca, *Nucleic Acids. Res.* **2016**, *44*, 1909–  
17 1923.